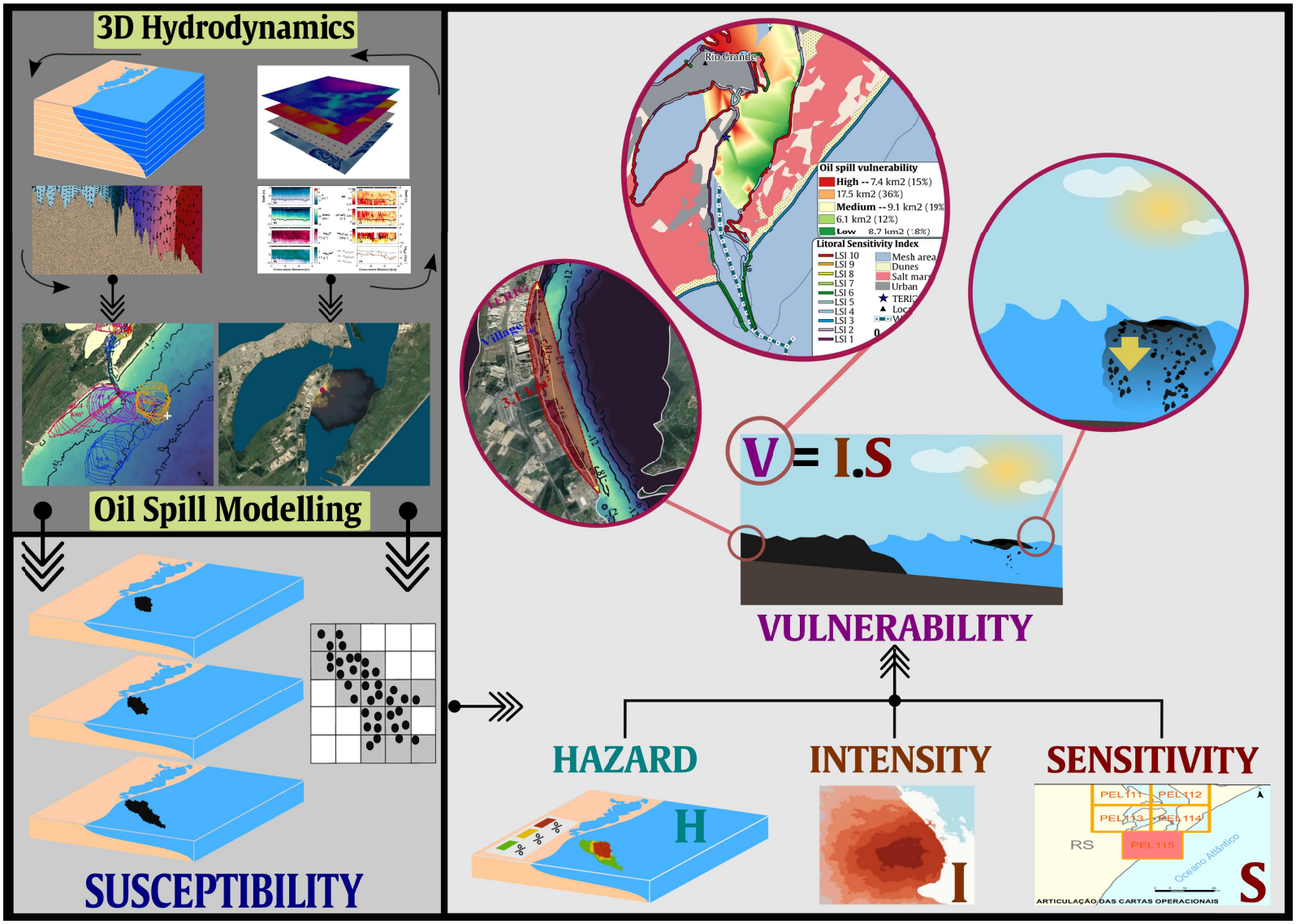
3D Hydrodynamics
Oil Spill Modelling
SUSCEPTIBILITY
Rio Grande
Oil spill vulnerability
High -- 7.4 km2 (15%)
17.5 km2 (36%)
Medium -- 9.1 km2 (19%
6.1 km2 (12%)
Low 8.7 km2 (18%)
Litoral Sensitivity Index
LSI 10
LSI 9
LSI 8
LSI 7
LSI 6
LSI 5
LSI 4
LSI 3
LSI 2
LSI 1
Mesh area
Dunes
Salt mar
Urban
V= I.S
VULNERABILITY
HAZARD
INTENSITY
SENSITIVITY
H
I
S
PEL 111
PEL 112
PEL 113
PEL 114
PEL 115
RS
Oceano Atlântico
ARTICULAÇÃO DAS CARTAS OPERACIONAIS

Integrated environmental vulnerability to oil spills in sensitive areas

Caroline Barbosa Monteiro[a,*], Phelype Haron Oleinik[b], Thalita Fagundes Leal[b], Wiliam Correa Marques[c], João Luiz Nicolodi[a], Bruna de Carvalho Faria Lima Lopes[d]

[a] *Postgraduate Program in Oceanology, Institute of Oceanography, Federal University of Rio Grande, Rio Grande, RS, Brazil*
[b] *School of Engineering, Federal University of Rio Grande, Rio Grande, RS, Brazil*
[c] *Institute of Mathematics, Statistics and Physics, Federal University of Rio Grande, Rio Grande, RS, Brazil*
[d] *Civil and Environmental Engineering Department, University of Strathclyde, Glasgow, Scotland, United Kingdom*

Abstract

As the typical range of influence of oil spills surrounds urbanised and economically active areas, it is likely that fragile regions may not be part of the most vulnerable zones. This premise is remediated in this paper with the adoption of a vulnerability approach based on the integration of static and dynamic information, such as oil pollution susceptibility. Susceptibility is a poorly consolidated term and is often used as synonym for environmental sensitivity; it is considered here to be the distribution areas of oil slicks. To test the proposed approach, an integrated estimation of environmental vulnerability is carried out for an environmentally sensitive area in the south of Brazil by merging static data inherent to the medium with information of a dynamic nature related to trajectory, behaviour and the fate of oil at sea. Moreover, the oil pollution intensity and environmental sensitivity data in susceptible areas are addressed. Subsequently, the environmental vulnerability is estimated by integrating hazard maps, concentrations and losses of the mass of the oil slick, oil beaching time and the littoral sensitivity index hierarchy. Results will prove to be useful to highlight critical areas for which the highest levels of severity are expected, which can lead to improvements in decision-making processes to support oil-spill prevention, as well as improve response readiness, especially in developing countries that have historically under-protected their sensitive regions.

Keywords: Oil spill modelling, susceptibility, environmentally sensitive, hazard, vulnerability,

Main finding

This study allowed us to estimate oil spill vulnerability in environmentally sensitive areas, which are the subject of high global concern due to environmental losses and other negative impacts.

1. Introduction

A vulnerability analysis of marine oil spills remains useful and important, mainly due to the fact that oil exploration and extraction continue to be large contributors in the global market (Nelson and Grubesic, 2018). According to classic approaches, oil spill vulnerability represents a measure of the degree of losses for the environmental elements in the face of the consequences of oil spills (Michel et al., 1978; Gundlach and Hayes, 1978; Hanna, 1995; Douglas, 2007; Williams et al., 2008). This information is usually obtained from oil sensitivity mappings that are represented as static variables (Nelson et al., 2015; Nelson and Grubesic, 2018; Amir-Heidari et al., 2019). On the other hand, physical vulnerability is defined as a dynamic variable that results from the integration of intrinsic environment data from other sources (Li et al., 2012; Uzielli et al., 2008). Information such as the fractions of oil evaporated and oil trapped on the coast can also be considered in estimations and classifications of vulnerable areas (Alves et al., 2015). Zones under oil spill risk may have

*Corresponding Author

greater or lesser vulnerability, despite the environmental levels of sensitivities among other conditioning factors (Alves et al., 2014, 2015; Nelson et al., 2015; Goldman et al., 2015; Guo et al., 2019). For example, a high oil-sensitive area, such as a salt marsh, can be less vulnerable than fine sand beaches, considering that the exposure levels of an oil spill are beyond coastal sensitivity levels. This is because oil sensitivity is inherent to the environment, which may be less or more sensitive depending on its own characteristics, while in contrast, physical vulnerability depends on external factors, such as oil covering levels and concentrations and oil beaching time in sensitive areas. Another concept that is sometimes mistakenly used as a synonym for environmental vulnerability is environmental sensitivity. Whereas environmental vulnerability derives from the susceptibility to an event of negative consequences (for Standardization , ISO) and could also be assumed to be a metric of the probability of exposure to external factors (Zacharias and Gregr, 2005), environmental sensitivity is assumed to be an intrinsic property of exposed elements (Guo et al., 2019).

Thus, vulnerability mapping comprehends an interdisciplinary evaluation and takes information from distinct scientific domains into account (Alves et al., 2016a,b; Shami et al., 2017). These maps are extremely important to decision-makers when planning for marine protected areas, placing new infrastructure or enacting protocols on handling marine pollution (Alves et al., 2016b; Goldman et al., 2015). The mapping of environmental vulnerability associated with marine oil spills has generally been supported more by information inherent to the environment than by the results of modelling the behaviour of oil in water. This, in turn, may lead to an imprecise evaluation of the extent of damage caused by accidents. Therefore, this study proposes an integrated assessment of environmental vulnerability based on a combination of static and inherent variables in the environment, and those related to the behaviour and dynamics of oil slicks. This work is aimed at estimating the possible reach of oil spills by indicating the most vulnerable areas, and consequently to monitoring expected damage in regions of the highest pollution probabilities. Figure 1 presents the main concepts covered by this paper and how they relate to the proposed approach for this integrated estimation of environmental vulnerability.

As illustrated Figure 1, vulnerability is understood here to be the expected degree of loss of exposed elements in the face of a potentially harmful event and disaster reduction (UN/ISDR, 2004). This concept not only essentially depends on the resistance of the exposed elements, but also on the potential of an accident (Salter, 1997; Kleissen et al., 2007). Thus, as highlighted in previous research (e.g., Goldman et al. (2015, 2017); Nelson et al. (2015); Nelson and Grubesic (2018)), the estimate of the environmental vulnerability to oil spills merges information of different natures, such as probability, intensity or severity of a spill, among other inputs. These considerations allow the determination of the scope of the effects of an oil spill, as well as a notion of the extension of the damage (Afenyo et al., 2016; Xu et al., 2019).

Following a well-accepted concept in the literature, a hazard is the probability of occurrence of a potentially damaging phenomenon in a given area and in a given period, and the impact of that event on the environment or society (Larson, 2003; Varnes, 1984). In this study, the hazard was measured as the oil-covering probabilities due to the movement and behaviour of hypothetical oil slicks in alertness areas. In case of accidental marine oil spills, shorelines with high hazard and sensitivity should be prioritised, as they are critical areas for pollution (Alves et al., 2014, 2015). An estimation of oil-susceptible areas can be employed to delimit hazard regions by indicating areas of spreading and diffusion of oil spills.

According to this paper's approach, a coast with absolutely no structures for handling fuels or oil tankers could have its integrated environmental vulnerability drastically reduced, even though the susceptibility, threat and intensity of oil spills are only considered from a theoretical point of view. Such an approach is useful in the context of many developing countries like Brazil, where the fact that a coastal zone is sensitive does not ensure that it is protected; to the contrary, many of these areas are the targets of significant damage caused by oil spills (Chun et al., 2020; Guo et al., 2019; Prasad et al., 2019; Oriaku et al., 2017; Salim et al., 2015; Na et al., 2012; Orta-Martínez and Finer, 2010). The case of the oil spill that recently hit several sectors of the Brazilian coast is a prime example of these weaknesses. Oil slicks were first identified on the Brazilian coast on August 30, 2019; they reached about 4,334 km of the coast and covered areas in 11 states of the Northeast and Southeast. The disaster is considered the worst marine oil spill in the history of Brazil and one of the largest ever recorded in the world (de Araújo et al., 2020; Pena et al., 2020).

Thus, the proposed integrated vulnerability approach allows representation of different levels of potential harm caused by the interaction between oil and the environment. Furthermore, it can improve the decision-

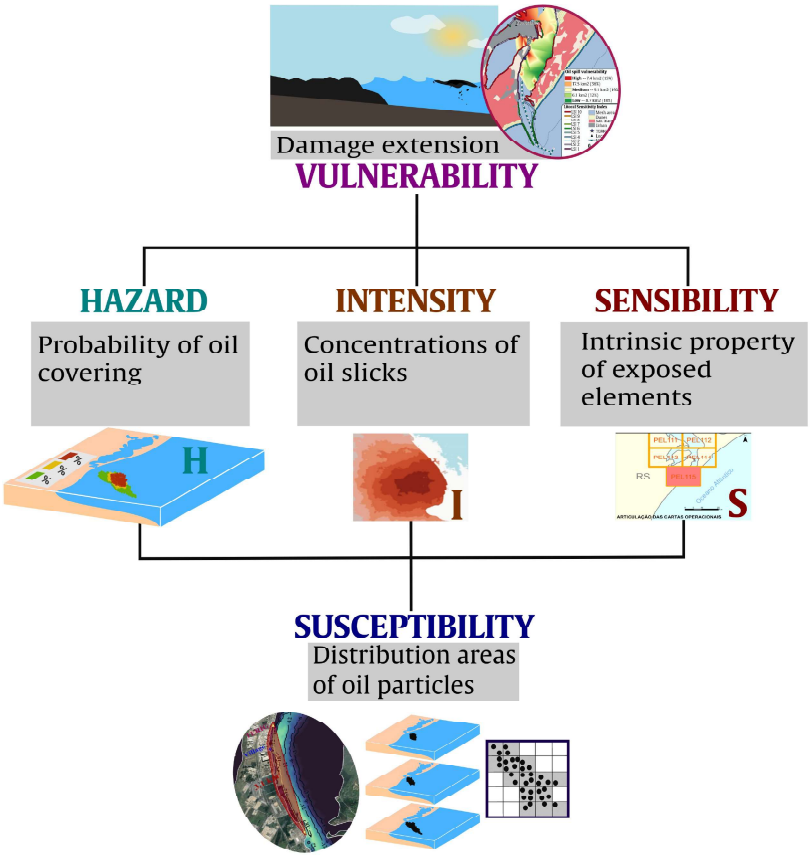

Figure 1: Proposed methodology involving the main extension of damages concepts to estimate integrated environmental vulnerability to oil spills.

making process for operators, responders and stakeholders to support oil-spill prevention and response readiness (Nelson et al., 2015). Additionally, this vulnerability estimating is useful to assess a range of conditions and scenarios and to provide a better understanding of the potential risks related to marine oil spills.

2. Materials and Methods

Numerical simulations of oil spill events were performed in order to estimate the probability of the studied areas to be polluted by oil in case of accidental spills. A total of 17.382 different scenarios were simulated, each characterised by the spill event's proximity to different possible pollution sources, such as shipping routes, pipelines and refinery and petrochemical industries. The oil covering probabilities were estimated using numerical modelling data. The oil spill simulations were carried out by coupling two numerical models, TELEMAC-3D and Easy Coupling Oil System (ECOS).

The methodological steps of this section can be summarised as follows:

I. Bathymetric, shoreline, oceanographic, meteorological and river discharge data were processed and interpolated to the computational grid, since they are key for TELEMAC-3D to generate the hydrodynamic results used in the oil-spill model.

II. The movement and behaviour of the oil spill and the susceptible areas were obtained from the ECOS model. For the weathering, it was used the time series of evaporation and emulsion mass in the first 48 h after the accidents, as well as for mass loss and oil beaching time data.

III. Oil-spill-susceptible areas were analysed and the probability of pollution was mapped using *TerraView*[1].

IV. The modelled data, the oil spill probabilities and the environmental oil sensibility data and spill behaviour were processed and integrated into a GIS environment using QGIS[2], and the Analytic Hierarchy Process (AHP) devised by Saaty (1990) was used to finally obtain the vulnerability areas.

A more thorough description of the dataset, computational grid independence tests, calibration of hydrodynamic parameters and validation of the simulation setup were previously performed and presented by (Monteiro et al., 2019a,b).

2.1. Study area

The Southern Brazilian Shelf (SBS, Fig. 2a) was selected as the study area due to historical records of accidental oil spills in its estuarine and coastal environments. Extending from latitude 34° S to 22° S, it is a wide continental shelf with intense coastal currents and large mesoscale variability generated by bathymetric and meteorological factors, such as local winds, micro-tidal behaviour and the constant influence of weather fronts, which are stronger during the winter (Stech and Lorenzzetti, 1992; Möller Jr et al., 2001; Dereczynski and Menezes, 2015). In terms of oil sensitivity, which is represented by the Littoral Sensitivity Index (LSI), this region presents rocky shores, which are classified as features of low coastal sensitivity to oil (LSI 1 and 2), sandy beaches (LSI 4 to 6) and sandy or muddy plains with vegetated margins classified according to specific characteristics (LSI of 8–10) (Marinho[1] and Nicolodi, 2019; Nicolodi, 2016; MMA, 2007). Most northern areas present a medium sensitivity to the influence of oil, except for some high– LSI areas around coastal lagoons. In the south, LSI values are more diverse, and more severe oil sensitivity levels can be found.

In the southern zone of the study area, the Patos Lagoon estuary is an economically important area for the southern Brazilian states due to maritime, industrial and tourism activities (Fig. 2b). This area is also threatened by pollution effects from the Rio Grande port and industrial zones, because of the activities of the oil refinery and the port terminal, fertiliser-production plants, fisheries and urban places in Rio Grande (Mirlean et al., 2003a,b; Lopes et al., 2019; Leal et al., 2019). At the northern region, the vicinities of

[1] http://www.obt.inpe.br/OBT/assuntos/projetos/terralib-terraview
[2] https://www.qgis.org

Tramandaí and Imbé are subjected to accidental spills at the oil collector buoy MN-602 (Fig. 2c), which connects the Almirante Soares Dutra Oceanic Terminal (TEDUT) to the Alberto Pasqualini Refinery (Refap) in Porto Alegre (Stringari, 2013; Monteiro et al., 2017; Marques et al., 2017). This locale poses an additional oil response challenge because oil spills can occur anywhere along the vessel routes, which makes it difficult to monitor the impact thereof.

2.2. Coupling between ECOS and Telemac*-3D*

The Telemac-3D hydrodynamic model was used to solve the hydrostatic Navier–Stokes equations under Boussinesq approximation, along with transport equations for scalar quantities of salinity and temperature. The finite element method was employed to solve the hydrodynamic equations, using sigma coordinate system for the vertical discretisation to represent both sea surface height and bed (Hervouet, 2007). Results from the three-dimensional hydrodynamic model, such as currents, salinity and temperature fields, were used by the ECOS oil-spill model to calculate the weathering processes and the transport of oil. ECOS represents an oil slick as a set of discrete particles, the displacement and properties of which are updated at each time step and changes in oil properties and hydrodynamic conditions are considered (Mello et al., 2011; Stringari, 2013; Marques et al., 2017). ECOS computes the oil slick evaporation using the algorithms of Stiver and Mackay (1984), Fingas (1995, 1999), with empirical coefficients obtained from Lehr et al. (2002). For the emulsification process, ECOS uses a first-order differential equation from Mackay et al. (1980) to consider the maximum emulsification for a light type of oil and other empirical constants according to Mackay et al. (1982). Mass changes in the oil slicks are computed based on emulsification and evaporation. Previous studies have verified that ECOS's results are in agreement with technical reports that monitor real oil spill incidents in the same region (Monteiro et al., 2019b) and with similar studies using the same setup (Marques et al., 2017; Monteiro et al., 2017).

2.3. Oil spill scenarios

To examine the potential spatial distribution of marine oil spills on the Southern Brazilian Shelf (SBS), the probability of the oil spill pollution was estimated by assuming three points for the start of the hypothetical oil spills modelled for a total of 17,382 daily events over nine years of simulations (2007–2015).The initial volume (20 m^3) of spills was chosen based on cases that have already occurred in the region. Each spill event was simulated separately as a scenario in which the oil load is instantly released from a certain point and then drifts for 48 h; results were recorded every 30 min. For the initialisation of the oil spills, two points were selected in the south (Fig. 2b): one was located in the Rio Grande Port manoeuvring zone (ZP-19—32°14′2″ S and 51°58′5″ W), and the other was at Transpetro's Waterway Terminal (TERIG—32°3′21″ S and 52°3′12″ W) in the estuary. In the north zone, the coordinates of the MN-602 buoy (30°1′36″ S and 50°5′12″ W) were used (Fig. 2c) as the initialisation point. After sensitivity simulations that used different values for oil specific gravity in the study area (Monteiro et al., 2019a), it was decided not to vary the oil specific mass values, and to use a single API gravity of 33.8 (856 kg/m^3), which is the typical diesel fuel that is frequently handled and transported in the study region.

2.4. Oil hazard

Mapping of the oil covering was based on the delimitation of areas susceptible to simulated oil slicks in the nine years of analysis (2007–2015) and was properly calibrated and validated for hydrodynamic conditions (Monteiro et al., 2019a,b). Therefore, oil particle distribution areas for the 17,382 scenarios allowed an approximation of the spatio-temporal occurrence of these events. Each oil spill simulation used a set of 10,000 particles to discretise the oil slicks; this number of particles ensures that the oil pollution estimation depends on the patterns of physical force that dictates oil movement in water, rather than the volume of oil in each particle. The estimation of the probability of oil covering $P(x, y)$ was centred on the longitude x and latitude y of each element of the computational grid. As was suggested by Goldman et al. (2017), contamination is confirmed by the presence of at least one particle in the batch of 10,000 particles released. Thus, hazard maps were generated for all points in the computational domain that were hit by at least one particle at any simulation time step, divided by the total number of particles for each simulated scenario.A

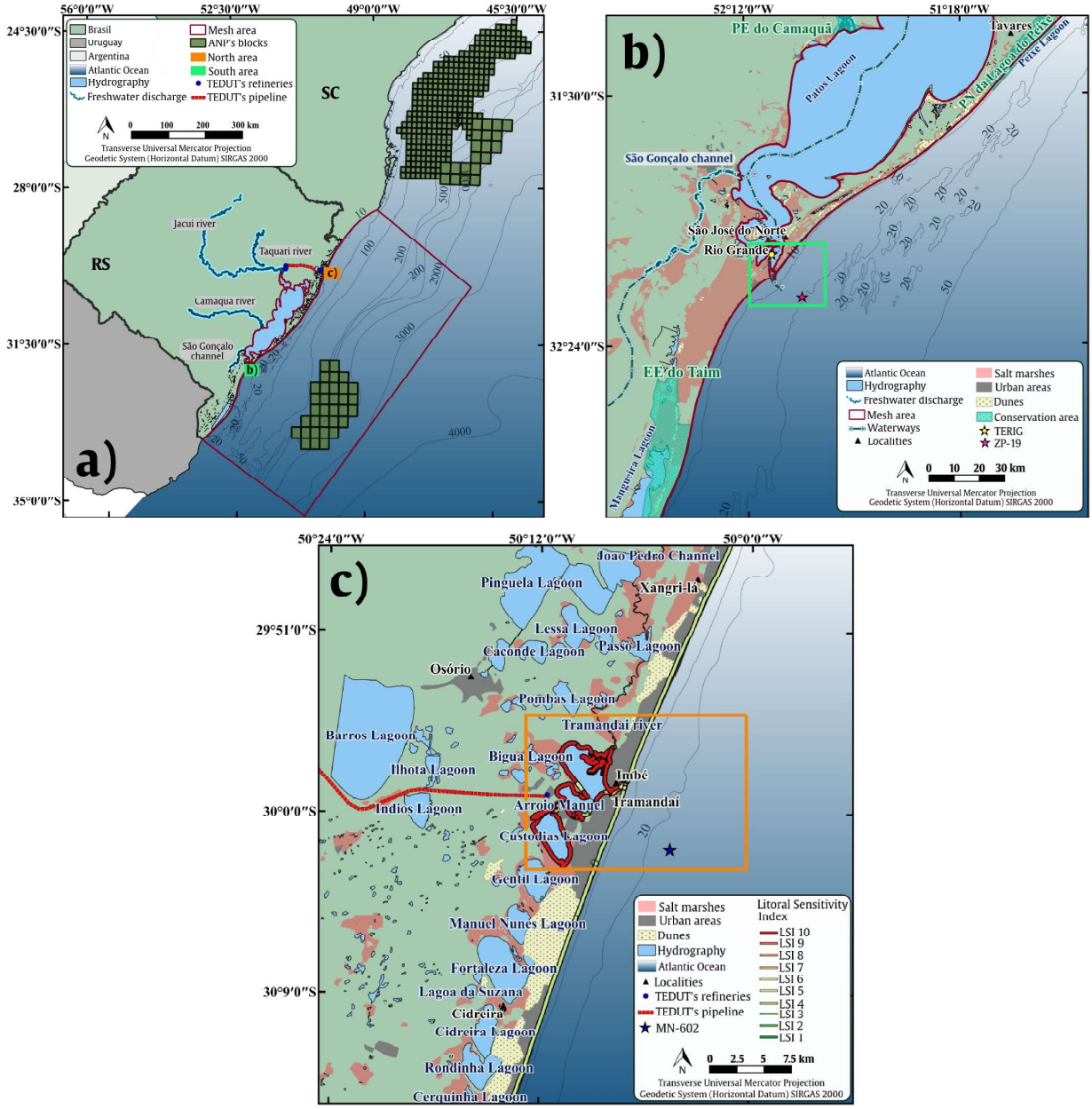

Figure 2: (a) The Southern Brazilian Shelf (SBS) and detail of the (b) south region of the study area: green box and star highlight estuarine and manoeuvring zone near the lagoon access channel respectively; and the (c) north region of the study area: orange box, with blue star highlighting the buoy near the coast.

limitation of the methodology is that the probabilities of oil covering were not estimated by categorising the volume of oil accumulated in the studied area. Therefore, this form of analysis may have overestimated the vulnerability in some regions with a high probability of oil covering, even under low concentrations.

The oil spilt at Patos Lagoon estuarine area is mainly driven by the strong estuarine currents, the dynamics of which essentially depend on wind and freshwater discharge levels (Möller Jr et al., 1996, 2001; Fernandes et al., 2001; Tavora et al., 2019), which leads to two main scenarios, flood and ebb currents.Thus, to better represent this dual flow, the analyses were conducted to consider separate oil spills under flood or ebb currents. To create better spatial orientation in the estuarine zone, the main critical oil sensitivity sectors were highlighted. It is worth pointing out that, even though these sectors had been recognised as ultra-sensitive areas, they did not receive any additional weight when estimating their integrated environmental vulnerability. The environmental sensitivity of these ultra-sensitive areas was weighted in the same way as all other areas assessed in this study (i.e., according to their ISL). The Kernel Probability Map concept (Mahmoodi and Sayedi, 2015) was used to measure the oil pollution probability for the study region as a matrix with a fixed number of rows and columns. The rows are related to the number of kernels in a window, the columns are related to the number of bins for each kernel, and each pixel is related to one kernel. In this study, a 5,000 × 5,000 window was assumed; thus, 25,000,000 kernels were possible. A quartic function and adaptive radius were used with SIG techniques and kernel maps in *TerraView* (Alves et al., 2019; Ferreira and Nascimento, 2019; Gehlen et al., 2019). These parameters were selected based on the works of Alves et al. (2019); Ferreira and Nascimento (2019); Gehlen et al. (2019) and were adapted according to the susceptibility area dimensions that resulted from the oil spill simulations. A probability function was estimated for each kernel, which allowed the calculation of each of those. Values of the probability for oil pollution, which are specified between 0 (0 % probability) and 1 (representing the maximum oil coverage), were considered for all 17,382 simulated oil spills.

2.5. Littoral Sensitivity Index Information

The LSI from the Brazilian Oil Sensitivity Charts (SAO charts) for Pelotas Basin (MMA, 2007; Nicolodi, 2016) were used to obtain oil sensitivity information. The LSI classifies the coastlines according to an environmental sensitivity scale that ranges from 1 as the lowest sensitivity to 10 as the highest sensitivity. This index considers the levels of exposure to wave and tidal energy, the slope of the coast and the type of substrate (Jensen et al., 1998; Petersen et al., 2002; Wieczorek et al., 2007). The study area was classified based on LSI at 1:50,000 scale (PEL101, PEL109–PEL115[3]). Then the study area was hierarchised in five levels of severity; the weight in zones with the highest LSI values, such as environmental conservation areas, urban zones next to fisheries and touristic areas, were increased.

2.6. Vulnerability classification

Hazard maps that contained the probability of oil covering, the LSI information and marine oil spill intensity levels were combined and integrated using GIS techniques in QGIS to estimate vulnerability.

Based on previous works (e.g., Zafirakou et al. (2018); Ha (2018); Nelson and Grubesic (2018); Alves et al. (2016a); Nelson et al. (2015)), after selecting six criteria related to oil vulnerability, pairwise comparisons were used to calculate priorities using Analytic Hierarchy Process (AHP) analysis, following the methodology of Saaty (1990). This generated 15 pairwise comparisons (Tab. 1) according to the matrix with the AHP priorities, and ranked which criterion was more important on a scale from 1–9. This pairwise matrix was reliable and presented a Consistency Ratio (CR) of 0.002 as defined by Saaty (1990). The highest weight values were assigned to important infrastructures, touristic sites, and highly sensitive coastal regions, due to their morphology and environmental structure.

For visualisation purposes, the vulnerability scores were classified into five categories that corresponded to different vulnerability levels: high (two levels: > 75 % and 50–75 %), medium (25–50 %) and low (two levels: 15–25 % and < 15 %); these were adapted from Nelson et al. (2015).

[3] www.mma.gov.br/seguranca-quimica/cartas-de-sensibilidade-ao-oleo/base-de-dados.html

Table 1: Factors and pairwise comparisons used to calculate priorities of the AHP. AHP Scale: 1⋆–Equal Importance, 3–Moderate importance, 5–Strong importance, 7–Very strong importance, 9–Extreme importance (2, 4, 6, 8: values in-between).

Factors	Priority (%)	Rank		**1**	**2**	**3**	**4**	**5**	**6**
Probability of oil covering	28	1	**1**	1⋆	1	1	5	6	5
Oil slick concentration	28	1	**2**	1	1⋆	1	5	6	5
LSI levels	28	1	**3**	1	1	1⋆	5	6	5
Evaporation rates	5.4	4	**4**	0.2	0.2	0.2	1⋆	1	1
Emulsion mass	5.0	6	**5**	0.17	0.17	0.17	1	1⋆	1
Oil beaching time	5.4	4	**6**	0.2	0.2	0.2	1	1	1⋆

3. Results and Discussions

An integrated oil spill vulnerability could be useful to mitigate oil spreading within few hours of its onset, before wind and currents disperse the slick (Alves et al., 2016b). Such data can also guide response protocols to prioritise the protection of critical areas. The simulated spills in estuarine region presented similar behaviour to that found in the results of previous studies for this area (e.g., Janeiro et al. (2008); Monteiro et al. (2006); Stringari et al. (2012); Lopes et al. (2019); Leal et al. (2019)). Hence, existing data of salinity, current velocity and wind direction were analysed along cross-sections in the estuarine region, which allowed the distinction of oil spills occurring under ebb or flood flows throughout the navigation channel and the inner shelf next to the starting point of spills (Fig. 3).

Under dominant ebb conditions, the oil has a longitudinal dispersion and reaches larger areas, is both deeper and shallower (Fig. 3b, d) and spread towards both inland regions and entrance of the access channel. On the other side, oil spills under flood conditions (Fig. 3a, c) led to a higher probability distribution of oil pollution over inland estuarine areas. For these two hydrodynamic conditions, the oil spill scenarios agreed with the results of previous works (e.g., Tomazelli (1993); Möller Jr et al. (1996); Möller and Castaing (1999); Möller Jr et al. (2001); Tavora et al. (2019)).

Due to the action of northeastern (NE) winds (Fig. 3b) in higher frequencies, ebb flows promote lagoon flux in a maritime direction (Fig. 3d), which is associated with high river discharges in situations where NE winds dominate, especially during winter and spring. Such settings favour the movement of oil slicks along the navigation channel. As presented in Fig. 3a and c, beyond the contribution of NE winds, contributions of strong southeast (SE) and southwest (SW) winds also increase the oil dispersion into shallower and estuarine areas under flood conditions. Here, the oil covering probabilities can reach such localities as the Franceses Bridge (P2) and Mangueira Bay (P3), both of which have significant environmental and economic importance to the region.

Different uses of water and resources in these areas can be affected. As an example, oil spills can jeopardise the artisanal fishery in this region, which has existed since the end of the 19$^{\text{th}}$ century and is still the main source of income for some communities (Pereira and D'Incao, 2012), supporting about 6,000 families throughout the coastline of Rio Grande do Sul state (Kalikoski et al., 2002). The studied Patos Lagoon estuary is an important environment for the life cycle of many fish, mollusc and crustacean species, notably because of its role as a sheltered area that allows their development from early larval stages (Castello, 1985; Muelbert et al., 2008; Vieira et al., 2008)) and offers an abundance of food (e.g., zooplankton) and protection from predators (Martins et al., 2007). These sheltered areas are also frequently used for fishing (D'Incao, 1991) and for the growth of estuarine juvenile pink shrimp and fishes (Vianna and D'Incao, 2006; Oliveira and Bemvenuti, 2006; Benedet et al., 2010).

According to Fig. 3, even though the radius of pollution can be extended to further areas, such as Torotama Island (P7), the highest oil pollution probabilities are near the Franceses Bridge (P2), Mangueira Bay (P3), New Harbor (P4), Marinheiros Island (P6) and the city of São José do Norte (P8).

As described by Alves et al. (2016a), these oil distribution probability scenarios can trigger more damages, since sheltered areas from the open sea often trap large quantities of oil, which worsens pollutions scenarios. Besides, salt-marshes and other highly vegetative locations with high LSI values are not only critical areas

because they are the most productive aquatic environments, but also because they are difficult to clean up and oil particles can persist in these places for years (Gundlach and Hayes, 1978; Heflin and Wallace, 2017; Marinho[1] and Nicolodi, 2019). Diversely, under prevailing NE and SW local winds, high continental freshwater supply (Fig. 3b and d) of predominant ebb conditions cause the highest pollution probabilities to remain in the middle of the estuary.

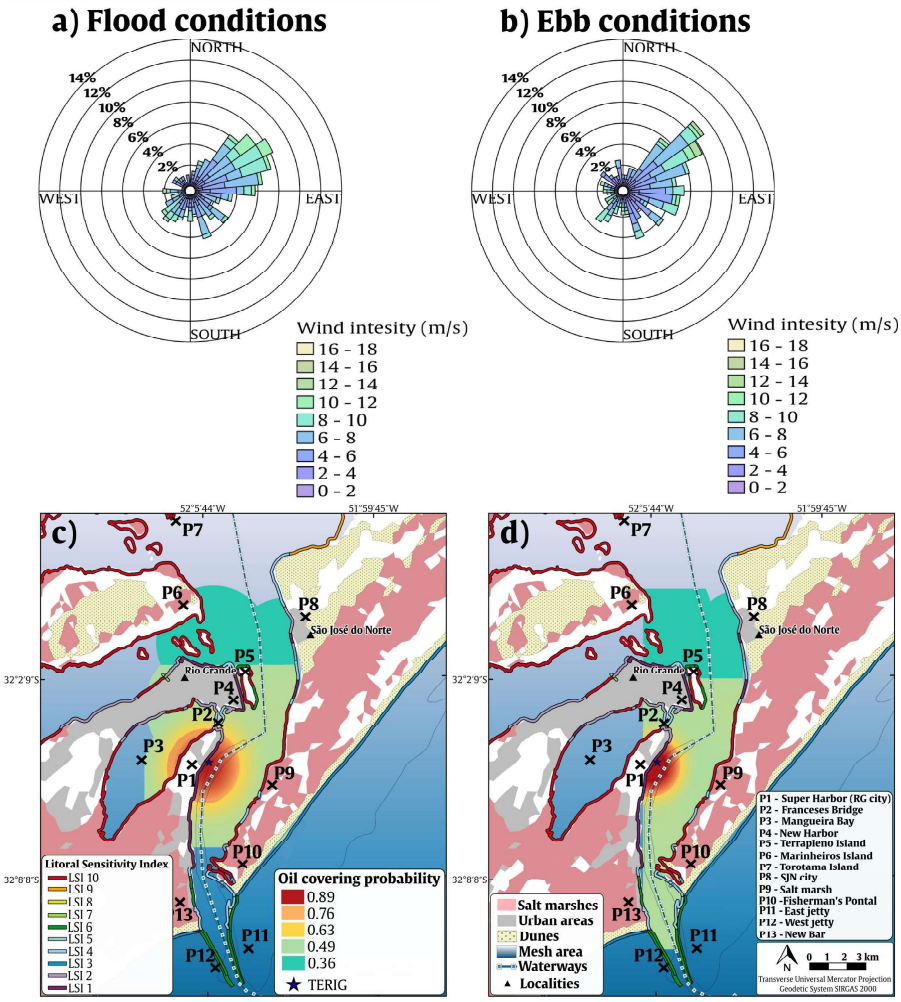

Figure 3: Probabilities for the estuarine area: under flood (a: wind velocity; c: hazard) and ebb (b: wind velocity; d: hazard).

Under flood flows, winds from the SW that are associated to east (E) and northwest (NW) quadrant currents contribute to the oil displacement over a large area. In this case, the hazard probabilities were also verified, both in the estuarine interior and in the portions closest to the lagoon inlet. Oil reached areas with varying levels of oil sensitivity, namely the Franceses Bridge (P2), Mangueira Bay (P3), New Harbor (P4), Marinheiros Island (P6), São José do Norte (P8), Torotama Island (P7) and vicinities of the lagoon entrance channel (P10–P13). In these cases, the most susceptible areas are those next to the Rio Grande port (P1) in a region near the oil release point due to the fast oil arrival time of an average of one hour to the nearby coastal structures.

In both scenarios, areas such as Fisherman's Pontal (P10) and the jetties (P11, P12) — especially the east jetty (P12) — were under hazard due to an increased interest in the conservation of marine species, such as pinnipeds (Kinas et al., 2005). Despite being distant from the oil release point, these locations were also susceptible to being covered by oil, with a probability of 0.49. Furthermore, these areas presented features,

such as salt marshes, coastal lagoons, bays and natural reserves, which cause them to be more susceptible to oil trapping.

For oil spills that started at the nearby continental shelf, a set of susceptibility areas to oil effects resulted in a greater spreading of areas likely to be contaminated (Fig. 4a). The highest hazard probabilities (i.e., values between 0.89–0.72) were confined to the smallest area in the vicinities of the Patos Lagoon inlet, and also overlapped important beaches in the region (Cassino & Barra de São José do Norte beaches) when winds and currents disperse them. Critical areas as the east jetty (P12) presented the highest oil-coverage probability (i.e., 0.89).

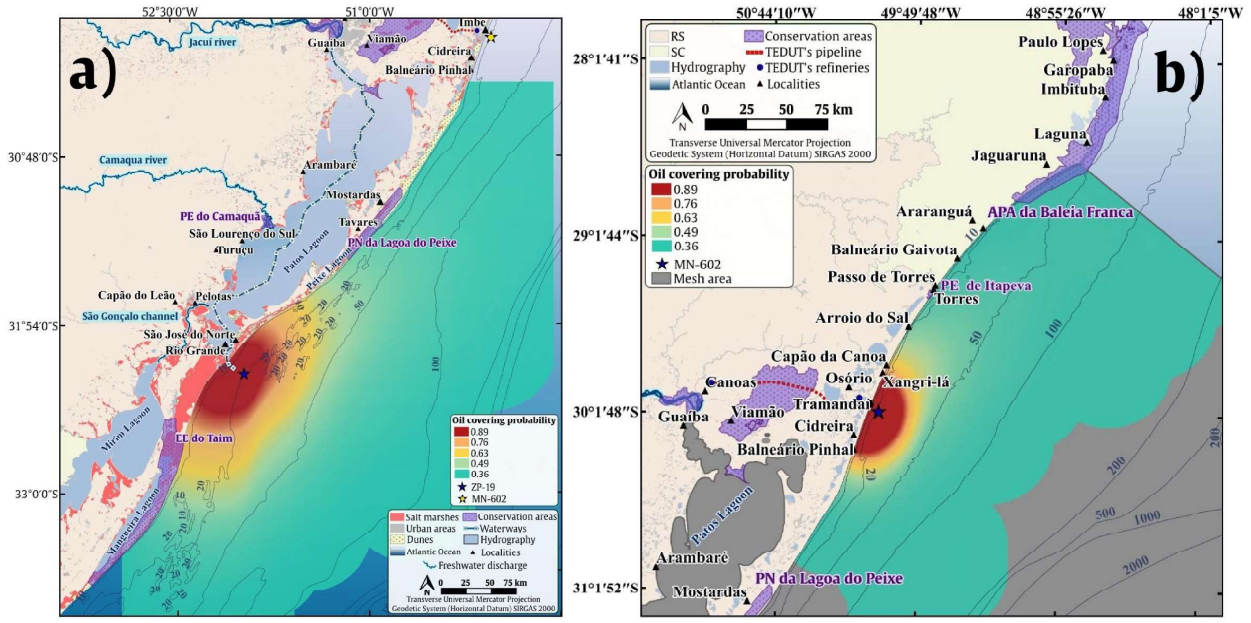

Figure 4: Oil covering hazard for (a) the manoeuvring zone near the lagoon access channel (ZP-19) and (b) the oil collector buoy (MN-602).

Despite this, the inherent danger of oil dispersal in this shore face has resulted in several threats over a wide area. Even though there were relatively low pollution probabilities (from 0.49–0.36), oil particles still reached environmental conservation sites, such as the Taim Ecological Reserve and the Lagoa do Peixe National Park. Meanwhile, this location is important to freshwater distribution that comes from Patos Lagoon and has environmental relevance because it forms an oceanfront mass of low-dynamic waters; this low-dynamic flow area was discussed in previous works (e.g., Soares et al. (2007a,b)). These results show that in the vicinities of Patos Lagoon plume, there is a tendency for high stratification at the lagoon discharge point. A low stratification area is then formed around it, and finally, high stratification values are found at the offshore border of the plume. This configuration helps the formation of a low-dynamic flow area in the inner shelf of the Lagoon plume, which plays an important ecological role (Soares et al., 2007a).

As presented in Fig. 4a, the highest probabilities of oil covering (i.e., 0.89–0.63) reached localities with relevant ecological functions and touristic importance. Beaches and fishing points can be jeopardised by oil spills in these regions (Terceiro, 2017, 2018), which threaten coastal lagoons, beaches, dunes and salt marshes. Although under lower pollution probabilities (i.e., 0.49), the effects of spill cases for the north point can hit long extensions along the SBS and reach conservation areas like Peixe Lagoon National Park and the whales environmental protection area (i.e., APA Baleia Franca) at the northern end of the computational grid.

For the three starting points studied, the potential hazards of these accidents were based on the calculation of a variable capable of predicting the presence and absence of oil particles within a given mapping unit. Thus, different features, such as strips of beaches, shorelines, coastal lagoons and salt marshes, were analysed. Concerning the vulnerability mapping, the challenge of the analysis was to identify regions with different

potential harm when faced with the impact of an oil spill. This step was preceded by calculations of oil dispersion areas, which also indicated how oil slicks spread and behave within different affected environments.

Different weights were attributed to LSI values so that the highest oil sensitive levels received the highest weights because they portrayed more critical situations. This weighting increased the vulnerability level of areas that had high concentrations of surface oil, while the weight was reduced for coastal and shelter areas with low LSI. Finally, as it relates to oil-covering probability, the LSI values and the spill intensity received equally high weights (i.e., 28 %—Tab. 1). All weighted factors were proportionally relevant to classify the study area in terms of vulnerability. This justifies, for example, the reasons why the areas with the highest oil-covering probability do not necessarily correspond to the most vulnerable areas.

For the estuarine oil spill starting points, two conditions of vulnerability were estimated; one was predominantly in flood conditions (Fig. 5a) and another was under ebb flow (Fig. 5b). When observing the differences between the vulnerability mapping for the same area, it was a possible to consider the relevance of physical forces, such as weather and oceanographic conditions, that work as a background to condition the movement, fate and behaviour of oil spill accidents.

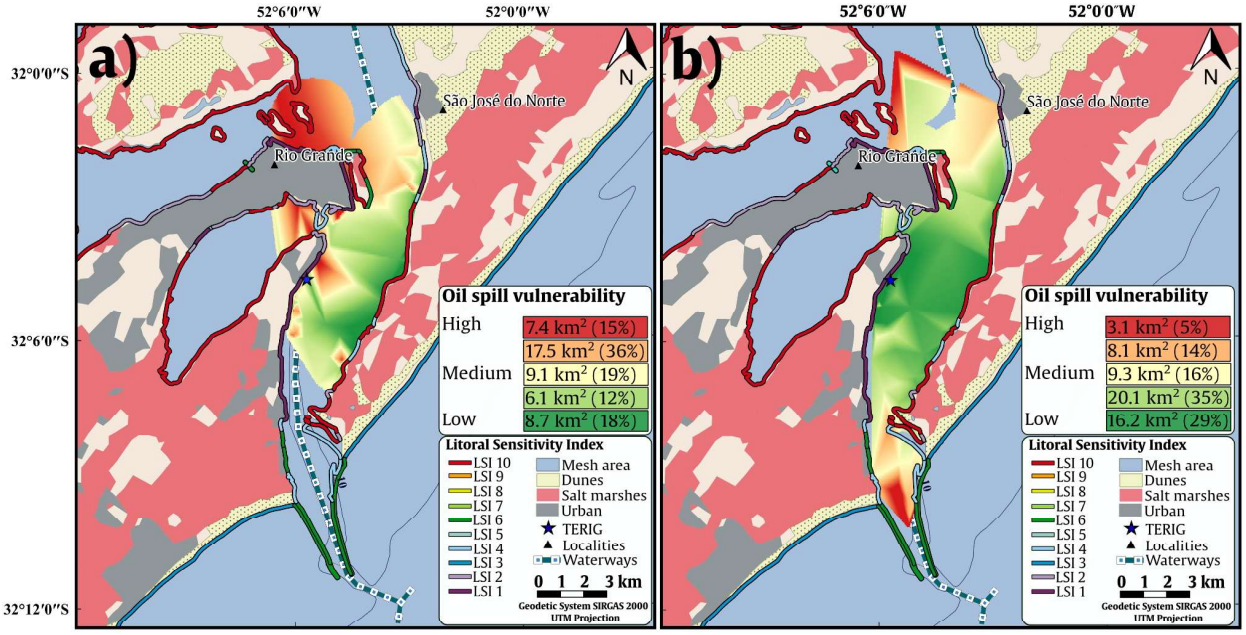

Figure 5: Vulnerability of oil spills started on the estuarine area under (a) flood and (b) ebb flow conditions.

Under more frequent autumn and winter winds (S and SW) that are associated with lower river discharges, flood flows predominate and favour saline wedge entrance from the inlet towards the innermost portions of the Patos Lagoon estuary. This flux also forces the superficial current velocities that conduct oil slick movement together with flood currents to become more prominent for these extreme hydrodynamic conditions (Fig. 5a). The scenario presented in Fig. 5a also showed areas with high vulnerability levels that represent about 51 % of the total area mapped (24.9 km^2), with high oil-sensitive areas in internal sections of the lagoon, such as Terrapleno, Marinheiros and Torotama Island.

Under ebb flows (Fig. 5b), the oil slicks spread along wider areas, and only about 19 % (11.2 km^2) of them present the highest vulnerability score, followed by another portion with a medium level of vulnerability (16 %—9.3 km^2). Hence, both of these areas are the most critical because of their greater vulnerability. Thus, a possible strategy to provide more urgent responses is to concentrate civil protection teams in these critical areas.

With an opposite effect, Fig. 5a shows the flood conditions, in which oil vulnerability area distribution is mainly ruled by estuarine currents forced by remote and local wind effects (i.e., the NE quadrant with higher frequencies) and high river discharges. These areas occur towards the inlet zone and generate oceanographic

fronts that are freshwater plumes over the heavier salty waters of the shoreface. Here, the vulnerable areas tend to be limited to salt marshes, bays and other sensitive areas for the biologic reproduction of local species and fishing activities. Under this flow condition, the highly vulnerable areas were less frequent (5 %) due to the major oil slick dispersion, despite the total area of 56.71 km^2 of vulnerable regions.

For the nearby continental shelf, the vulnerability areas were spread out, representing an area of 35,937 km^2 (Fig. 6), the largest among the modelled scenarios. This spreading is probably due to stronger action of currents and local wind effects that condition the local hydrodynamics. About 23 % (8,323 km^2) of the total vulnerable areas correspond to the highest scores; most are located next to the most sensitive areas with severe conditions of oil-covering probability.

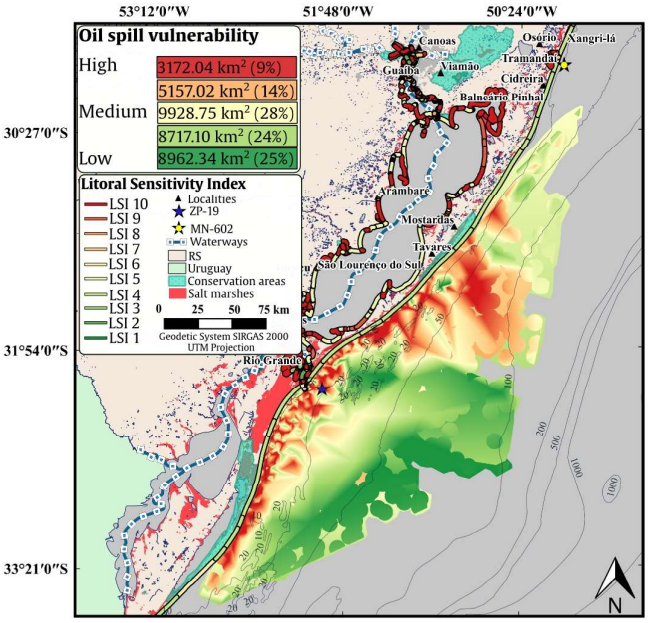

Figure 6: Vulnerability to oil spills started in the manoeuvring zone near the lagoon access channel (ZP-19).

Additionally, previous studies in this region reported the accumulation of spawning fish and plankton next to the lagoon access channel, which emphasises that the low dynamic in this area is an important feature for fish spawning and larval development (Soares et al., 2007a). For these reasons, accidental oil spills are a severe potential threat in these areas, especially in regions with oceanographic fronts like the studied region, due to the Patos Lagoon plume also being capable of dragging oil slicks, thereby jeopardising different species of local fauna and local activities of economic and social importance.

For the northern scenarios, about 28 % of these vulnerable areas (5,123 km^2) correspond to high levels of severity to oil slick exposures (Fig. 7). In addition to beaches, coastal lagoons located within about 30 % of the littoral zones (Nicolodi, 2016) also showed high vulnerability to oil spills. Coastal lagoons in this area have a depth ranging from 1–2 m, which allows sunlight to penetrate the entire water column. This situation is favourable for the development of algae, which is the food base for fish and crustaceans, making this region a natural nursery for these species (Cotrim and Miguel, 2007). Therefore, environmental hazards that arise from oil spills in this region can lead to both ecological and economic losses (Terceiro, 2017), similar to what happened in a recent and severe oil spill in shallow areas on the Brazilian coast (de Araújo et al., 2020; Pena et al., 2020). As was verified by Terceiro (2017, 2018), the region's fishing activities are in conflict with the oil industry. According to the author, the vulnerability of fishing resources and the fisherman economy is high with respect to oil enterprises in which the buoy considered by the study is located. Considering the mapping of the types of fishing in the region and the results of the present study, areas of greater vulnerability (from high to medium), which extend over about 41 % of the mapped area (7,441.63 km^2), are confronted with sport, boat and net fishing.

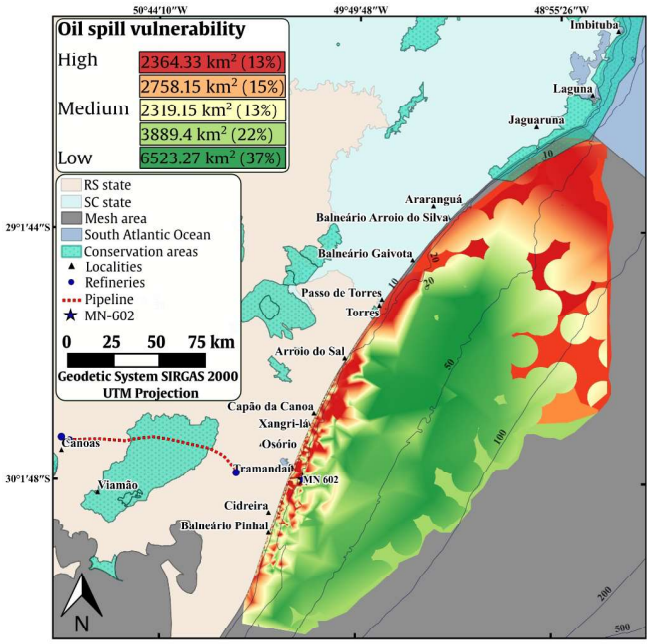

Figure 7: Vulnerability to oil under spills started on the buoy MN-602 point, near the Tramandaí coastal zone.

Moreover, the present vulnerability mapping can predict the pollution of fragile areas about which Alves et al. (2015) warned, and salt marshes and coastal lakes can draw water from foreshore areas polluted with oil, thereby contaminating sub-surface aquifers and soil for a long time after an oil spill. These findings can improve oil spill response in sensitive areas, based both on static mapping information for expeditious measurements, such as SAO chart work, and actions that consider dynamic variables integrated with the characterisation of the environment involved in oil spill cases. Furthermore, the classification of areas based on the vulnerability levels thereof can optimise civil protection management by promptly directing efforts into critical areas (Alves et al., 2016a).

In addition, the results agree such classical works as (Gundlach and Hayes, 1978) and (Hanna, 1995), since the vulnerability concept allows determination of which coastal environmental would be more seriously damaged by oil contamination so that they can receive priority protection. Urgent responses in high-vulnerability areas are important to anticipate the costs of oil spill responses, as was presented by Etkin (2000), because costs are estimated in terms of the affected area and the degree of shoreline fragility, among other variables. Thus, as the resources and equipment for oil contingency actions are usually limited, these results can help to mitigate major oil spill accidents and the undesirable effects thereof on marine environment.

4. Conclusions

The aim of this paper was to improve the body of knowledge concerning an integrated vulnerability assessment for oil spills in sensitive areas by incorporating modelled data, oil covering hazard probability and littoral sensitivity information, among other data related to marine oil spill behaviour. The modelling system utilised consisted of coupling a 3D hydrodynamic model (i.e., TELEMAC-3D) with an oil-spill model (i.e., ECOS) and employing the results from global meteorological and oceanographic models as boundary conditions. A set of 17,382 oil spills performed along nine years of simulations (2007–2015), together with information on environmentally sensitive elements of oil effects, made the estimation of areas susceptible to oil spills possible.

The results showed that circulation patterns have a strong influence on the oil-covering probability and vulnerability estimates. The enhanced methodology allowed: (1) accurate base maps to be consulted whenever a marine oil spill case occurred in an environmentally sensitive region; (2) a detailed estimation of

susceptible and vulnerable areas; (3) the use of a relational GIS database to store and integrate information on oil-sensitive areas, shorelines, bays, coastal lagoons and estuarine features; and (4) the identification of oil-pollution-critical areas when the origin of the simulated spill is close to shipping routes, pipelines, gas wells, single-buoy moorings and other oil-spill-risk sources.

In addition, the outputs of this study can inform the process of systematic planning in the event of oil spills. The identification of priority areas for response actions can maximise the achievement of conservation goals while minimising the expected threats and losses. Furthermore, the vulnerability scenarios can be used as a background to recommend possible cleaning and containment methods. Finally, these findings can help guide pollution-control actions in areas under greater vulnerability, thereby prioritising timely interventions in sensitive areas in the aftermath of oil-spill accidents.

5. Funding

This study was partially financed by Coordenação de Aperfeiçoamento de Pessoal de Nível Superior Brasil (CAPES) and has Finance Code 001. We thank the resources provided by CAPES to support the Postgraduate Program in Oceanology. The authors also acknowledge the support of the CNPq and FAPERGS for sponsoring the research (contracts 304227/2016-1 and 17/2551-0001159-7).

6. Acknowledgements

The authors wish to thank the Brazilian Navy and GEBCO for the bathymetric dataset, ANA for the fluvial discharge data and ECMWF and HYCOM for the global reanalysis datasets. The authors would also like to thank the Open Telemac-Mascaret Consortium for the free distribution of Telemac-3D to the Federal University of Rio Grande (FURG) for the ECOS model and the National Supercomputing Center (CESUP) and the National Laboratory of Scientific Computing (LNCC) for allocating time for the use of their supercomputer systems.

References

J. R. Nelson, T. H. Grubesic, Oil spill modeling: Risk, spatial vulnerability, and impact assessment, Progress in Physical Geography: Earth and Environment 42 (2018) 112–127. doi: 10.1177/0309133317744737.

J. Michel, M. O. Hayes, P. J. Brown, Application of an oil spill vulnerability index to the shoreline of lower cook inlet, alaska, Environmental Geology 2 (1978) 107–117. doi: 10.1007/bf02380473.

E. R. Gundlach, M. O. Hayes, Vulnerability of coastal environments to oil spill impacts, Marine Technology Society Journal 12 (1978) 18–27.

R. G. Hanna, An approach to evaluate the application of the vulnerability index for oil spills in tropical red sea environments, Spill Science & Technology Bulletin 2 (1995) 171–186. doi: 10.1016/s1353-2561(96)00016-3.

J. Douglas, Physical vulnerability modelling in natural hazard risk assessment, Natural Hazards and Earth System Science 7 (2007) 283–288.

J. M. Williams, M. L. Tasker, I. C. Carter, A. Webb, A method of assessing seabird vulnerability to surface pollutants, Ibis 137 (2008) S147–S152. doi: 10.1111/j.1474-919x.1995.tb08435.x.

J. Nelson, T. Grubesic, L. Sim, K. Rose, J. Graham, Approach for assessing coastal vulnerability to oil spills for prevention and readiness using GIS and the blowout and spill occurrence model, Ocean & Coastal Management 112 (2015) 1–11. doi: 10.1016/j.ocecoaman.2015.04.014.

P. Amir-Heidari, L. Arneborg, J. F. Lindgren, A. Lindhe, L. Rosén, M. Raie, L. Axell, I.-M. Hassellöv, A state-of-the-art model for spatial and stochastic oil spill risk assessment: A case study of oil spill from a shipwreck, Environment International 126 (2019) 309–320. doi: 10.1016/j.envint.2019.02.037.

L. Li, J. Wang, H. Leung, S. Zhao, A bayesian method to mine spatial data sets to evaluate the vulnerability of human beings to catastrophic risk, Risk Analysis: An International Journal 32 (2012) 1072–1092. doi: 10.1111/j.1539-6924.2012.01790.x.

M. Uzielli, F. Nadim, S. Lacasse, A. M. Kaynia, A conceptual framework for quantitative estimation of physical vulnerability to landslides, Engineering Geology 102 (2008) 251–256. doi: 10.1016/j.enggeo.2008.03.011.

T. M. Alves, E. Kokinou, G. Zodiatis, R. Lardner, C. Panagiotakis, H. Radhakrishnan, Modelling of oil spills in confined maritime basins: The case for early response in the eastern mediterranean sea, Environmental Pollution 206 (2015) 390–399. doi: 10.1016/j.envpol.2015.07.042.

T. M. Alves, E. Kokinou, G. Zodiatis, A three-step model to assess shoreline and offshore susceptibility to oil spills: The south aegean (crete) as an analogue for confined marine basins, Marine Pollution Bulletin 86 (2014) 443–457. doi: 10.1016/j.marpolbul.2014.06.034.

R. Goldman, E. Biton, E. Brokovich, S. Kark, N. Levin, Oil spill contamination probability in the southeastern Levantine basin, Marine Pollution Bulletin 91 (2015) 347–356. doi: 10.1016/j.marpolbul.2014.10.050.

W. Guo, S. Zhang, G. Wu, Quantitative oil spill risk from offshore fields in the bohai sea, china, Science of The Total Environment 688 (2019) 494–504. doi: 10.1016/j.scitotenv.2019.06.226.

I. O. for Standardization (ISO), Risk management — vocabulary (iso guide 73:2009), Washington, DC: International Organization for Standardization Retrieved from https://www.iso.org/obp/standard 73 (2009) 1–15.

M. A. Zacharias, E. J. Gregr, Sensitivity and vulnerability in marine environments: an approach to identifying vulnerable marine areas, Conservation Biology 19 (2005) 86–97. URL: https://doi.org/10.1111/j.1523-1739.2005.00148.x. doi: 10.1111/j.1523-1739.2005.00148.x.

T. M. Alves, E. Kokinou, G. Zodiatis, R. Lardner, Hindcast, GIS and susceptibility modelling to assist oil spill clean-up and mitigation on the southern coast of cyprus (eastern mediterranean), Deep Sea Research Part II: Topical Studies in Oceanography 133 (2016a) 159–175. doi: 10.1016/j.dsr2.2015.07.017.

T. M. Alves, E. Kokinou, G. Zodiatis, H. Radhakrishnan, C. Panagiotakis, R. Lardner, Multidisciplinary oil spill modeling to protect coastal communities and the environment of the eastern mediterranean sea, Scientific Reports 6 (2016b). doi: 10.1038/srep36882.

A. A. Shami, G. Harik, I. Alameddine, D. Bruschi, D. A. Garcia, M. El-Fadel, Risk assessment of oil spills along the mediterranean coast: A sensitivity analysis of the choice of hazard quantification, Science of The Total Environment 574 (2017) 234–245. doi: 10.1016/j.scitotenv.2016.09.064.

UN/ISDR, Living with risk: A global review of disaster reduction initiatives, volume 1, United Nations Publications, 2004.

J. Salter, Risk management in a disaster management context, Journal of Contingencies and Crisis Management 5 (1997) 60–65. doi: 10.1111/1468-5973.00037.

F. Kleissen, L. Arentz, M. Reed, O. Johansen, Marine environmental risk assessment system: Conceptual design and preliminary demonstration for the dutch continental shelf: Demo a: inventory, classification and risk assessment of oil transport on the north sea, Z4339 (2007).

R. Goldman, R. Goldman, E. Biton, E. Biton, I. Gertman, I. Gertman, G. Zodiatis, G. Zodiatis, B. Herut, B. Herut, An evaluation of oil pollution probability in the Levantine Basin off Israel, in: Proceedings of International Conference "Managinag risks to coastal regions and communities in a changinag world" (EMECS-11 - SeaCoasts XXVI), Academus Publishing, 2017. doi: 10.31519/conferencearticle_5b1b93715e1b93.24235003.

M. Afenyo, B. Veitch, F. Khan, A state-of-the-art review of fate and transport of oil spills in open and ice-covered water, Ocean Engineering 119 (2016) 233–248. doi: 10.1016/j.oceaneng.2015.10.014.

J. Xu, Z. Hao, Y. Wang, J. Liu, G. Liu, Y. Zhang, Modeling and numerical simulation of oil spill at different positions of blunt body, in: 2019 3rd International Forum on Environment, Materials and Energy (IFEME 2019), Atlantis Press, 2019. doi: ifeme-19.2019.95.

E. Larson, Living with risk: a global review of disaster reduction initiatives, Diane Publishing Company, 2003.

D. Varnes, Landslide hazard zonation: a review of principles and practice, volume 3, Natural hazards, 1984.

J. Chun, J.-H. Oh, C.-K. Kim, Oil spill response policies to bridge the perception gap between the government and the public: A social big data analysis, Journal of Marine Science and Engineering 8 (2020) 335. doi: 10.3390/jmse8050335.

S. J. Prasad, P. A. Francis, T. M. B. Nair, S. S. C. Shenoi, T. Vijayalakshmi, Oil spill trajectory prediction with high-resolution ocean currents, Journal of Operational Oceanography 13 (2019) 84–99. doi: 10.1080/1755876x.2019.1606691.

T. O. Oriaku, N. A. Udo, I. S. Iwuala, Assessment of Oil Spill Occurrences in Sections of the Niger Delta Region: Causes, Effects and Remedial Actions, in: SPE Nigeria Annual International Conference and Exhibition, Society of Petroleum Engineers, 2017. doi: 10.2118/189090-ms.

M. Salim, R. Nayak, P. Mohanthy, S. Sasamal, V. Dadhwal, C. Dutt, M. Rao, Characterization of the seasonal circulation patterns and its application on oil spill transport in the northwestern continental shelf of india, Marine Geodesy 38 (2015) 241–260. doi: 10.1080/01490419.2015.1008709.

J. U. Na, M. S. Sim, I. J. Jo, H. G. Song, The duration of acute health problems in people involved with the cleanup operation of the hebei spirit oil spill, Marine Pollution Bulletin 64 (2012) 1246–1251. doi: 10.1016/j.marpolbul.2012.03.013.

M. Orta-Martínez, M. Finer, Oil frontiers and indigenous resistance in the peruvian amazon, Ecological Economics 70 (2010) 207–218. doi: 10.1016/j.ecolecon.2010.04.022.

M. E. de Araújo, C. W. N. Ramalho, P. W. de Melo, Artisanal fishers, consumers and the environment: immediate consequences of the oil spill in pernambuco, northeast brazil, Cadernos de Saúde Pública 36 (2020). doi: 10.1590/0102-311x00230319.

P. G. L. Pena, A. L. Northcross, M. A. G. de Lima, R. de Cássia Franco Rêgo, The crude oil spill on the brazilian coast in 2019: the question of public health emergency, Cadernos de Saúde Pública 36 (2020). doi: 10.1590/0102-311x00231019.

T. L. Saaty, An exposition of the AHP in reply to the paper "remarks on the analytic hierarchy process", Management Science 36 (1990) 259–268. doi: 10.1287/mnsc.36.3.259.

C. B. Monteiro, P. H. Oleinik, B. V. Lopes, T. F. Leal, O. O. Möller Jr, W. C. Marques, Oil spill simulations and susceptibility in coastal and estuarine areas, Defect and Diffusion Forum 396 (2019a) 109–120. doi: 10.4028/www.scientific.net/DDF.396.109.

C. B. Monteiro, P. H. Oleinik, B. V. Lopes, T. F. Leal, D. V. da Silva, O. O. Möller Jr, W. C. Marques, Reproducibility of a real case of an oil spill during vessel supply operation in an estuarine zone, Defect and Diffusion Forum 396 (2019b) 121–131. doi: 10.4028/www.scientific.net/DDF.396.121.

J. L. Stech, J. A. Lorenzzetti, The response of the South Brazil Bight to the passage of wintertime cold fronts, Journal of Geophysical Research: Oceans 97 (1992) 9507–9520. doi: 10.1029/92jc00486.

O. O. Möller Jr, P. Castaing, J. Salomon, P. Lazure, The influence of local and non-local forcing effects on the subtidal circulation of Patos Lagoon, Estuaries 24 (2001) 297–311. doi: 10.2307/1352953.

C. P. Dereczynski, W. F. Menezes, Meteorologia da bacia de campos, in: Meteorologia e Oceanografia, Elsevier, 2015, pp. 1–54.

485 doi: 10.1016/B978-85-352-6208-7.50008-8.
486 C. Marinho[1], J. L. Nicolodi, Integração de parâmetros geomorfológicos e biológicos no desenvolvimento do índice integrado de
487 sensibilidade do litoral (iisl), Revista Brasileira de Geografia Física 12 (2019) 1509–1524. doi: 10.26848/rbgf.v12.4.p1509-1524.
488 J. L. Nicolodi, Atlas de Sensibilidade Ambiental ao Óleo da Bacia Marítima de Pelotas, Ministério do Meio Ambiente, Secretaria
489 de Mudanças Climáticas e Qualidade Ambiental, Departamento de Qualidade Ambiental, Gerência de Qualidade Costeira e
490 do Ar, 2016.
491 MMA, Especificações e normas técnicas para a elaboração de Cartas de Sensibilidade Ambiental para derramamentos de óleo, 1
492 ed., Brasília, 2007.
493 N. Mirlean, V. E. Andrus, P. Baisch, Mercury pollution sources in sediments of Patos Lagoon estuary, Southern Brazil, Marine
494 Pollution Bulletin 46 (2003a) 331–334. doi: 10.1016/S0025-326X(02)00404.
495 N. Mirlean, V. E. Andrus, P. Baisch, G. Griep, M. R. Casartelli, Arsenic pollution in Patos Lagoon estuarine sediments, Brazil,
496 Marine Pollution Bulletin 46 (2003b) 1480–1484. doi: 10.1016/S0025-326X(03)00257.
497 B. V. Lopes, A. Pavlovic, T. B. Trombetta, P. H. Oleinik, C. B. Monteiro, R. C. Guimarães, D. V. da Silva, W. C. Marques,
498 Numerical Study of Oil Spill in the Patos Lagoon Under Flood and Ebb Conditions, Journal of Marine Science and Engineering
499 7 (2019) 4. doi: 10.3390/jmse7010004.
500 T. F. Leal, C. B. Monteiro, M. C. Silva, O. O. Möller Jr, P. H. Oleinik, W. C. Marques, Numerical study of oil spill in the patos
501 lagoon estuary region, Revista de Engenharia Térmica 18 (2019) 22. doi: 10.5380/reterm.v18i1.67026.
502 C. E. Stringari, The influence of winds and coastal currents on the oil spill event : Case study of Tramandaí Beach , 26 th January
503 2012, II Conferência Internacional em Tecnologias Naval e Offshore: Energia e Sustentabilidade - NAVTEC 2013 (2013).
504 C. B. Monteiro, E. d. P. Kirinus, W. C. Marques, P. H. Oleinik, J. Costi, Analysis of two oil spills in the Southern Brazilian Shelf,
505 in the years of 2012 and 2014, Defect and Diffusion Forum 372 (2017) 70–80. doi: 10.4028/www.scientific.net/DDF.372.70.
506 W. C. Marques, C. E. Stringari, E. P. Kirinus, O. O. Möller, E. E. Toldo, M. M. Andrade, Numerical modeling of the
507 Tramandaí beach oil spill, Brazil—case study for January 2012 event, Applied Ocean Research 65 (2017) 178–191. doi:
508 10.1016/j.apor.2017.04.007.
509 J. M. Hervouet, Free surface flows: modelling with the finite element methods, John Wiley & Sons, 2007. doi: 10.1002/
510 9780470319628.
511 L. F. Mello, C. E. Stringari, R. T. Eidt, W. C. Marques, Desenvolvimento de um Modelo Lagrangiano de Transporte de
512 Óleo: Estruturação e Acoplamento ao Modelo Hidrodinâmico TELEMAC-3D, in: P. Sausen (Ed.), Pesquisas Aplicadas em
513 Modelagem Matemática, volume 1, Editora Unijui, 2011, pp. 1–21.
514 W. Stiver, D. Mackay, Evaporation rate of spills of hydrocarbons and petroleum mixtures, Environmental Science and Technology
515 18(11) (1984) 834–840. doi: 10.1021/es00129a006.
516 M. F. Fingas, A literature review of the physics and predictive modelling of oil spill evaporation, Journal of Hazardous Materials
517 42 (1995) 157–175. doi: 10.1016/0304-3894(95)00013-k.
518 M. Fingas, The evaporation of oil spills: development and implementation of new prediction methodology, in: International Oil
519 Spill Conference, 1, American Petroleum Institute, 1999, pp. 281–287. doi: 10.7901/2169-3358-1999-1-281.
520 W. Lehr, R. Jones, M. Evans, D. Simecek-Beatty, R. Overstreet, Revisions of the ADIOS oil spill model, Environmental
521 Modelling & Software 17 (2002) 189–197. doi: 10.1016/S1364-8152(01)00064-0.
522 D. Mackay, B. K. Trudel, S. Paterson, C. E. I. C. Directorate, C. E. E. B. Research, D. Division, A Mathematical model of oil
523 spill behaviour, Research and Development Division, Environmental Emergency Branch, Canada, 1980.
524 D. Mackay, W. Y. Shiu, K. Hossain, W. Stiver, D. McCurdy, Development and calibration of an oil spill behavior Model,
525 Technical Report, Toronto University (Ontario) Dept of Chemical Engineering and Applied Chemistry, 1982.
526 O. O. Möller Jr, J. A. Lorenzzentti, J. Stech, M. M. Mata, The Patos Lagoon summertime circulation and dynamics, Continental
527 Shelf Research 16 (1996) 335–351.
528 E. H. Fernandes, K. R. Dyer, L. F. H. Niencheski, Calibration and validation of the TELEMAC-2D model to the Patos Lagoon
529 (Brazil), Journal of Coastal Research (2001) 470–488. doi: https://www.jstor.org/stable/25736313.
530 J. Tavora, E. H. L. Fernandes, A. C. Thomas, R. Weatherbee, C. A. F. Schettini, The influence of river discharge and wind on
531 Patos Lagoon, Brazil, Suspended Particulate Matter, International Journal of Remote Sensing 40 (2019) 4506–4525. doi:
532 10.1080/01431161.2019.1569279.
533 M. R. Mahmoodi, S. M. Sayedi, A face detection method based on kernel probability map, Computers & Electrical Engineering
534 46 (2015) 205–216. doi: 10.1016/j.compeleceng.2015.02.005.
535 L. S. Alves, D. T. dos Santos, M. A. M. Arcoverde, T. Z. Berra, L. H. Arroyo, A. C. V. Ramos, I. S. de Assis, A. A. R. de Queiroz,
536 J. B. Alonso, J. D. Alves, M. P. Popolin, M. Yamamura, J. de Almeida Crispim, E. M. Dessunti, P. F. Palha, F. Chiaraval-
537 Neto, C. Nunes, R. A. Arcêncio, Detection of risk clusters for deaths due to tuberculosis specifically in areas of southern
538 brazil where the disease was supposedly a non-problem, BMC Infectious Diseases 19 (2019). doi: 10.1186/s12879-019-4263-1.
539 F. R. Ferreira, L. F. C. Nascimento, Spatial approach of leprosy in the State of São Paulo, 2009-2012, Anais Brasileiros de
540 Dermatologia 94 (2019) 37–41. doi: 10.1590/abd1806-4841.20197351.
541 M. Gehlen, M. R. Nicola, E. R. Costa, V. K. Cabral, E. L. de Quadros, C. O. Chaves, R. A. Lahm, A. D. Nicolella, M. L.
542 Rossetti, D. R. Silva, Geospatial intelligence and health analitycs: Its application and utility in a city with high tuberculosis
543 incidence in Brazil, Journal of Infection and Public Health 12 (2019) 681–689. doi: 10.1016/j.jiph.2019.03.012.
544 J. R. Jensen, J. N. Halls, J. Michel, A systems approach to Environmental Sensitivity Index (ESI) mapping for oil spill
545 contingency planning and response, Photogrammetric Engineering and Remote Sensing 64 (1998) 1003–1014.
546 J. Petersen, J. Michel, S. Zengel, M. White, C. Lord, C. Plank, Environmental Sensitivity Index Guidelines. Version 3.0, NOAA
547 Technical Memorandum NOS OR&R 11 (2002) 1–192.
548 A. Wieczorek, D. Dias-Brito, J. C. C. Milanelli, Mapping oil spill environmental sensitivity in Cardoso Island State Park and
549 surroundings áreas, São Paulo, Brazil, Ocean & Coastal Management 50 (2007) 872–886. doi: 10.1016/j.ocecoaman.2007.04.007.

A. Zafirakou, S. Themeli, E. Tsami, G. Aretoulis, Multi-criteria analysis of different approaches to protect the marine and coastal environment from oil spills, Journal of Marine Science and Engineering 6 (2018) 125. doi: 10.3390/jmse6040125.

M. Ha, Modeling for the allocation of oil spill recovery capacity considering environmental and economic factors, Marine Pollution Bulletin 126 (2018) 184–190. doi: 10.1016/j.marpolbul.2017.11.006.

J. Janeiro, E. Fernandes, F. Martins, R. Fernandes, Wind and freshwater influence over hydrocarbon dispersal on Patos Lagoon, Brazil, Marine Pollution Bulletin 56 (2008) 650–665. doi: 10.1016/j.marpolbul.2008.01.011.

I. O. Monteiro, M. L. Pearson, O. O. M. Junior, E. H. L. Fernandes, Hidrodinâmica do saco da mangueira: mecanismos que controlam as trocas com o estuário da lagoa dos patos, Atlântica (Rio Grande) 27 (2006) 87–101. doi: 10.5088/atlÃćntica.v27i2.2175.

C. E. Stringari, W. C. Marques, L. F. Mello, R. T. Edit, Modeling the wind influence in an oil spill along the Southern Brazilian Shelf, Science Engenharia Térmica (Thermal Engineering) Engenharia Térmica (Thermal Engineering) 100 (2012) 100–109.

L. Tomazelli, O regime dos ventos e a taxa de migração das dunas eólicas costeiras do rio grande do sul, brasil, Pesquisas em Geociências 20 (1993) 18. doi: 10.22456/1807-9806.21278.

O. O. Möller, P. Castaing, Hydrographical characteristics of the estuarine area of patos lagoon (30 s, brazil), in: Estuaries of South America, Springer Berlin Heidelberg, 1999, pp. 83–100. doi: 10.1007/978-3-642-60131-6_5.

N. Pereira, F. D'Incao, Relationship between rainfall, pink shrimp harvest (farfantepenaeus paulensis) and adult stock, associated with el niño and la niña phenomena in patos lagoon, southern brazil, Journal of the Marine Biological Association of the United Kingdom 92 (2012) 1451–1456. doi: 10.1017/s0025315412000021.

D. C. Kalikoski, M. Vasconcellos, L. Lavkulich, Fitting institutions to ecosystems: the case of artisanal fisheries management in the estuary of patos lagoon, Marine Policy 26 (2002) 179–196. doi: 10.1016/s0308-597x(01)00048-3.

J. Castello, La ecologia de los consumidores del estuario de la Lagoa dos Patos, Brasil, Fish community ecology in estuaries and coastal lagoons: towards an ecosystem integration (1985) 383–406.

J. H. Muelbert, M. Acha, H. Mianzan, R. Guerrero, R. Reta, E. S. Braga, V. M. Garcia, A. Berasategui, M. Gomez-Erache, F. Ramírez, Biological, physical and chemical properties at the subtropical shelf front zone in the SW atlantic continental shelf, Continental Shelf Research 28 (2008) 1662–1673. doi: 10.1016/j.csr.2007.08.011.

J. P. Vieira, A. M. Garcia, A. M. Grimm, Evidences of el niño effects on the mullet fishery of the patos lagoon estuary, Brazilian Archives of Biology and Technology 51 (2008) 433–440. doi: 10.1590/s1516-89132008000200025.

I. Martins, J. Dias, E. Fernandes, J. Muelbert, Numerical modelling of fish eggs dispersion at the patos lagoon estuary - brazil, Journal of Marine Systems 68 (2007) 537–555. doi: 10.1016/j.jmarsys.2007.02.004.

F. D'Incao, Pesca e biologia de penaeus paulensis na lagoa dos patos, rs, Atlântica 13 (1991) 159–169.

M. Vianna, F. D'Incao, Evaluation of by-catch reduction devices for use in the artisanal pink shrimp (farfantepenaeus paulensis) fishery in patos lagoon, brazil, Fisheries Research 81 (2006) 331–336. doi: 10.1016/j.fishres.2006.06.011.

A. Oliveira, M. d. A. Bemvenuti, O ciclo de vida de alguns peixes do estuário da lagoa dos patos, rs, informações para o ensino fundamental e médio, Cadernos de ecologia aquática 1 (2006) 16–29.

R. A. Benedet, D. C. Dolci, F. D'Incao, Descrição técnica e modo de operação das artes de pesca artesanais do camarão-rosa no estuário da lagoa dos patos, rio grande do sul, brasil, Atlântica (Rio Grande) 32 (2010) 05–24. doi: https://doi.org/10.5088/atlÃćntica.v32i1.1549.

F. Heflin, D. Wallace, The BP oil spill: Shareholder wealth effects and environmental disclosures, Journal of Business Finance & Accounting 44 (2017) 337–374. doi: 10.1111/jbfa.12244.

P. G. Kinas, K. G. d. Silva, S. Estima, D. d. S. Monteiro, Generalized linear models applied to stranding data of south american sea lions (otaria flavescens) and south american fur seals (arctocephalus australis) in southern brazil, Latin American Journal of Aquatic Mammals 4 (2005) 7–14. doi: 10.5597/lajam00065.

I. D. Soares, V. Kourafalou, T. N. Lee, Circulation on the western south atlantic continental shelf: 1. numerical process studies on buoyancy, Journal of Geophysical Research 112 (2007a). doi: 10.1029/2006jc003618.

I. D. Soares, V. Kourafalou, T. N. Lee, Circulation on the western south atlantic continental shelf: 2. spring and autumn realistic simulations, Journal of Geophysical Research 112 (2007b). doi: 10.1029/2006jc003620.

A. M. Terceiro, Getting to know the artisan fishing in tramandaí and imbé - rs: space distribution and challenges, Ciência e Natura 39 (2017) 341–351.

A. M. Terceiro, The oil flow and artisan fishing in tramandaí and imbé - RS: an analysis in the context of environmental justice, Ciência e Natura 40 (2018) 8. doi: 10.5902/2179460x26248.

D. S. Cotrim, L. d. A. Miguel, Uso do enfoque sistêmico na pesca artesanal em tramandaí–rs, Eisforia 5 (2007) 136–160.

D. S. Etkin, Worldwide analysis of marine oil spill cleanup cost factors, in: Arctic and marine oilspill program technical seminar, volume 1, Environment Canada; 1999, 2000, pp. 161–174.